Supporting Information

Orthogonal Chain Collapse in Stimuli-responsive Di-block Polymers leading to Self-sorted Nanostructures

Chirag Miglani,[a] Maqsuma Banoo,[b] Debasish Nath,[a] Jahanvi Ralhan,[a] Soma Sil,[b] Jojo P. Joseph,[a] Santanu K. Pal,[b] Ujjal Gautam,[b] Asish Pal*[a]*

[a]*Chemical Biology Unit, Institute of Nano Science and Technology, Knowledge City, Sector 81, Mohali, Punjab, 140306 (India)*

[b]*Department of Chemical Sciences, IISER Mohali, Knowledge City, Sector 81, Mohali, Punjab*

Email: apal@inst.ac.in, ujjalgautam@iisermohali.ac.in

Table of Contents

1. Materials and methods

Solvents used in synthesis were of reagent grades. Acetone, dichloromethane, and 1-4 dioxane used were dried as per the literature protocol.[S1] The chemicals azobisisobutyronitrile (AIBN), 4-cyano-4-[(phenylcarbonothioyl)thio]pentanoic Acid (CTP), oxalyl chloride, coumarin, ferrocene were purchased from TCI chemicals and were used without further purification. 2-Hydroxy ethyl methacrylate (HEMA), was purchased from TCI and was passed through basic alumina (to remove inhibitor MEHQ) before using them for ATRP.[S2] Coumarin-2-hydroxy ethyl methacrylate (C-HEMA) and ferrocene-2-hydroxy ethyl methacrylate (F-HEMA) were synthesized according to literature procedure.[S3,S4]

^{1}H-NMR and 2D NMR spectra were acquired on a 400 MHz FT-NMR spectrometer model Avance Neo (Bruker). The chemical shifts were reported in ppm and appeared downfield to tetramethylsilane using the resonance of the deuterated solvent as an internal standard. Splitting patterns are designated as singlet (s), doublet (d), triplet (t) and multiplet (m).

Size exclusion chromatorgraphy (SEC) measurements were performed on the Malvern Omnisec instrument having RI detector using Shodex KD-806 M column and DMF as eluent (0.01M LiBr additive) with a flow rate of 0.7 mL/min at temperature of 35 ^{o}C. The results were analysed using Omnisec software with PMMA as the conventional calibration standard to result for M_n, M_w and *PDI*. The samples were prepared by filtering the solutions through a 0.2 μm nylon filter into a 2 mL glass vial.

Dynamic light scattering measurements were performed on Malvern Zetasizer Nano ZS ZEN3600 equipped with a Helium−Neon laser (wavelength, λ = 633 nm with backscattering angle of 173°. Samples were prepared by filtering solutions through a 0.2 μm nylone-filter into a glass cuvette.

UV crosslinking/decrosslinking was performed using an UV chamber equipped with 1* 8W UV_B lamp (λ_{max} = 320 nm, Intensity at 15 cm = 790 μW/cm^2) and 1*8W UV_C lamp (λ_{max} = 254 nm, Intensity at 15 cm = 820 μW/cm^2) and the sample in liquid state was kept at a distance of 15 cm for irradiation. Luminous intensity of irradiation at time *t* was determined in J/cm^2 by the formula **[(μW/cm^2)/10^6]*t (s)**. UV spectra were recorded using Agilent Cary 60 spectrophotometer in a wavelength range of 800 to 200 nm.

The sample was drop-cast on a 300 mesh carbon-coated copper grid with uranyl acetate as a staining agent and TEM images were recorded using (JEOL JEM-F200) with a Tungsten filament at an accelerating voltage of 200 kV.

Cyclic voltammetry (CV) studies were performed on Metrohm MULTI AUTOLAB M204 potentiostat/galvanostat using a standard three-electrode system.

Polymer monolayers were prepared using a KSV Nima Langmuir Blodgett trough that was placed horizontally within a Plexiglas box to avoid surface contamination. The surface pressure measurements were performed using a filter paper Wilhelmy plate. The trough was filled with an aqueous milli Q water. Polymer **P-*b*-C**, **P-*b*-F**, **P-*b*-C + P-*b*-F** dissolved in chloroform at a concentration of 1 mg/mL was added drop-wise on the surface Milli Q water. Chloroform was allowed to evaporate for 15 min after the addition of a known volume of polymer solution. The barriers were then allowed to compress symmetrically at a compression rate of 10 mm/min. The surface pressure versus area per molecule was obtained using KSV Nima software.

2. Synthesis and Characterization of the block copolymers:

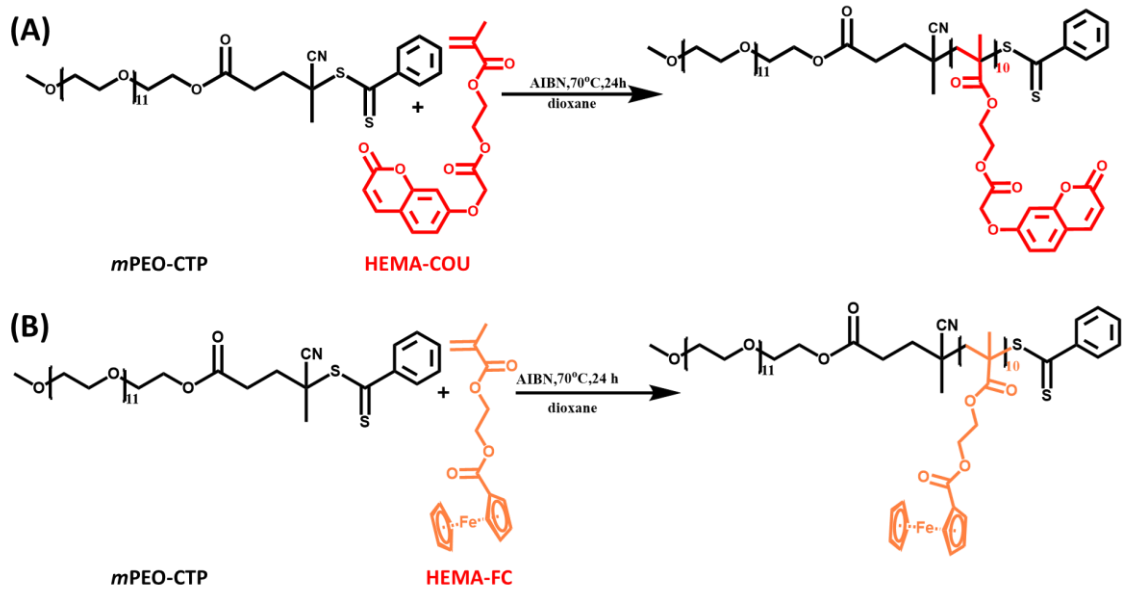

Scheme S1: Synthesis of (A) **P-*b*-C** and (B) **P-*b*-F** polymers using RAFT polymerization.

Synthesis of PEO_{11}-CTA:

The macro-RAFT agent, polyethylene oxide tethered with 4-cyano-4-[(phenylcarbonothioyl)thio]pentanoic acid (PEO_{11}-CTP) was designed by the esterification reaction of the hydroxy terminal in *m*PEO_{11}-OH with the carboxyl group in CTP following a literature protocol.[S5] Into a 100 mL flask, CTP (110 mg, 0.27 mmol) and DCM (2.0 mL) were

taken with subsequent dropwise addition of oxalyl chloride (157 mL, 2.5 mmol) dissolved in DCM (1 mL) for 10 min under nitrogen atmosphere. The mixture was magnetically stirred at 25 ^{o}C for about 2 h until the gas evolution stopped. The solvent and the excess oxalyl chloride were removed by rotary evaporation. Then *mPEO*$_{11}$-OH (100 mg, 0.18 mmol) dissolved in DCM (2 mL) was added to the solution and was allowed to stir for 24 h at 25 ^{o}C under inert atmosphere. The solution was concentrated under reduced pressure, and the polymer was precipitated in *n*-hexane and dried in a vacuum oven at room temperature to afford the desired macro-RAFT agent of *mPEO*$_{11}$-CTP (141.5 mg, 96% yield).

Synthesis of diblock Polymer (P-*b*-C):

Polymer (**P-*b*-C**) was synthesized through RAFT polymerization: The monomer, coumarin-2-hydroxy ethyl methacrylate (80 mg, 0.24 mmol), *mPEO*$_{11}$-CTP (20 mg, 0.024 mmol) and the initiator azobisisobutyronitrile (AIBN) (4 mg, 0.024 mmol) were taken in 1.5 mL dioxane. The solution mixture was degassed by N_2 bubbling followed by stirring at room temperature under inert environment for 24 h. Then the product was precipitated in cold ether followed by the centrifugation to furnish a white precipitate that was dried *in vacuo* to yield **P-*b*-C** (70 mg, 70%).

^{1}H NMR (400 MHz, $CDCl_3$, 298 K) δ = 7.56 (br s, 6 H), 7.32 (br s, 7 H), 6.82 (br s, 14 H), 6.16 (br s, 6 H), 4.75 (br s, 13 H), 4.4-3.8 (br s, 37 H), 3.79-3.66 (m, 54 H), 2.26 (br s, 22 H), 1.94 (br s, 6H).

SEC (DMF/LiBr, PMMA standards) M_n = 4663, M_w = 5796, *PDI* = 1.4.

Synthesis of diblock Polymer (P-*b*-F)

Polymer (**P-*b*-F**) was synthesized through RAFT polymerization: The monomer, ferrocene-2-hydroxy ethyl methacrylate (118 mg, 0.35 mmol), *mPEO*$_{11}$-CTP (28 mg, 0.035 mmol) and initiator AIBN (10 mg, 0.074 mmol) were taken in 1.5 mL dioxane. . The solution mixture was degassed by N_2 bubbling followed by stirring at room temperature under inert environment for 24 h. Then the product was precipitated in cold ether followed by the centrifugation to furnish a white precipitate that was dried *in vacuo* to yield **P-*b*-F** (100 mg, 68%).

^{1}H NMR (400 MHz, $CDCl_3$, 298 K) δ = 7.52 (t, 2H), 7.35 (t, 1H), 7 (br s, 2 H), 4.42 (br s, 33 H), 4.20 (br s, 44 H), 3.6-3.72 (m, 29 H), 3.4-3.52 (m, 51 H), 1.18-128 (m, 57 H).

SEC (DMF/LiBr, PMMA standards) M_n = 4477, M_w = 6771, *PDI* = 1.5.

3. ^{1}H NMR characterization of the polymers ($CDCl_3$, 400 Hz):

P-*b*-C

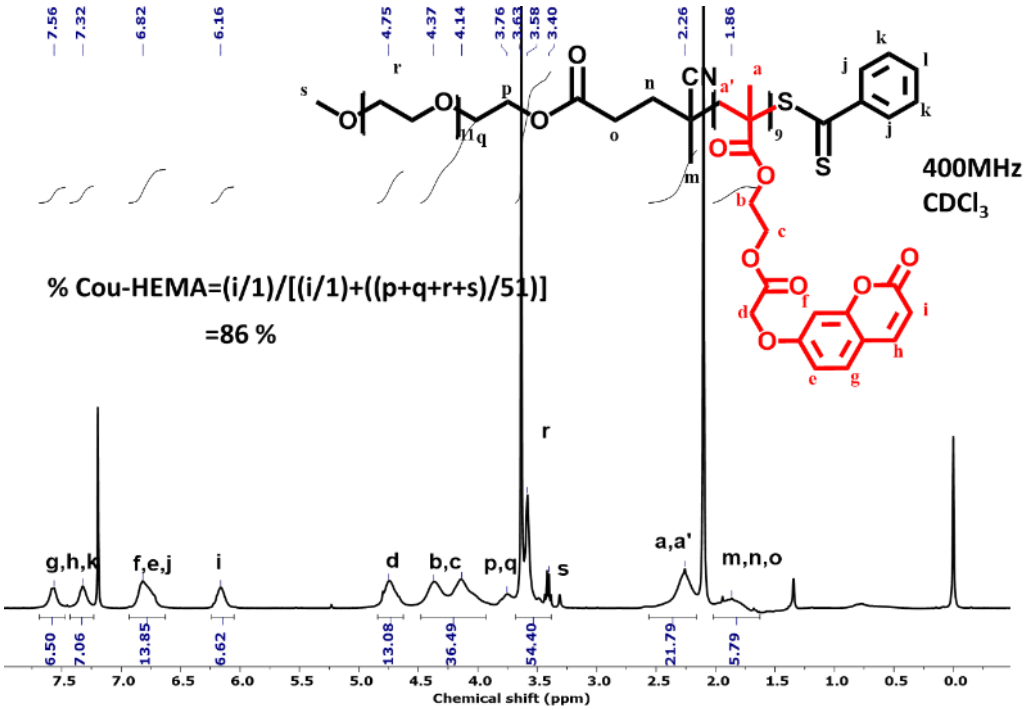

P-*b*-F

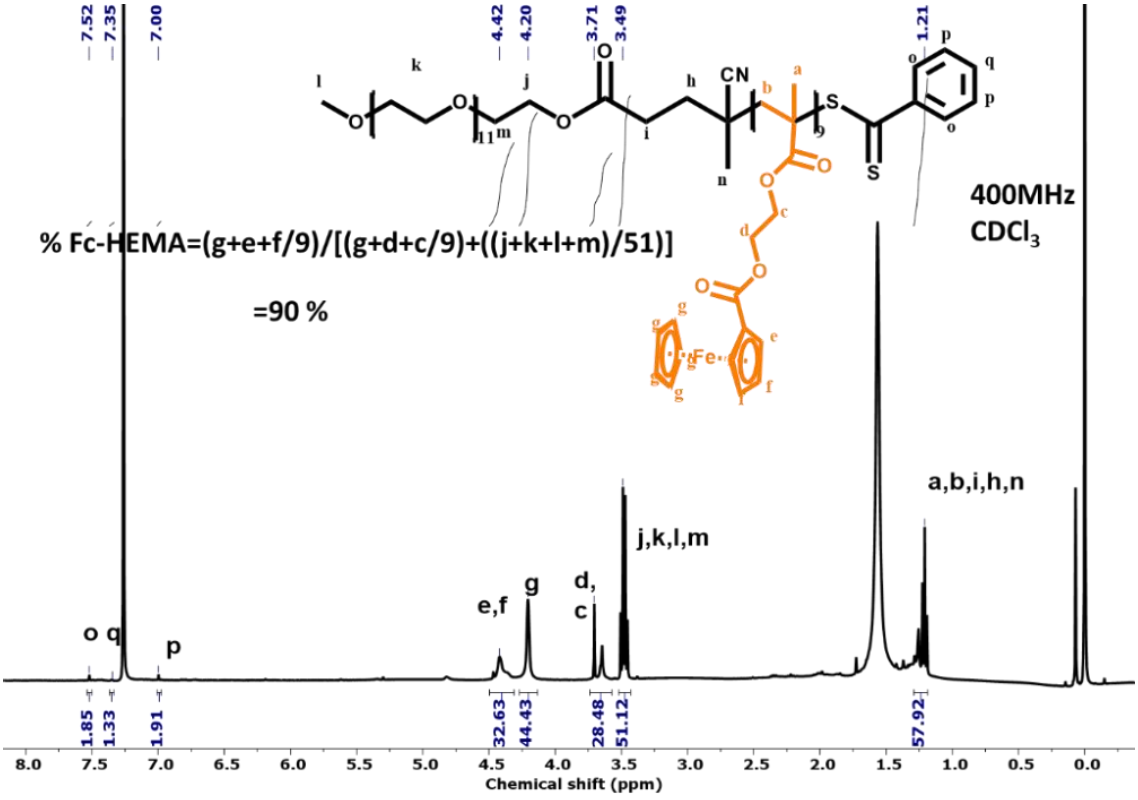

4. Size exclusion chromatography of the polymers:

All the polymer samples were dissolved at a concentration of 5 mg/mL in DMF and were shaken for 2-3 h in order to ensure complete solubility of the polymers. The sample solution was then filtered through nylon syringe filter while adding to the vial. 100 µL of the samples were injected and run at a flow rate of 0.7 mL/min for 30 min.

P-*b*-C

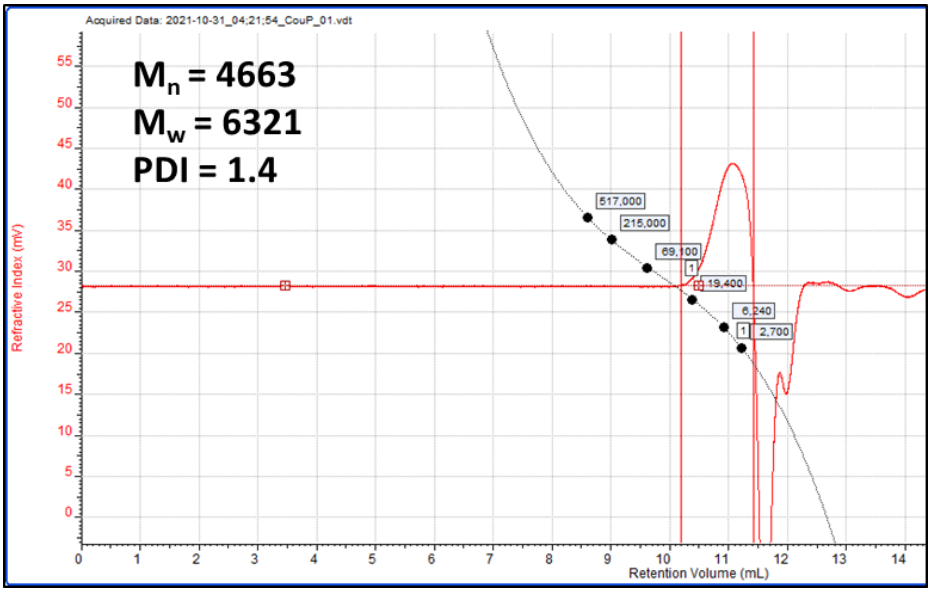

P-*b*-F

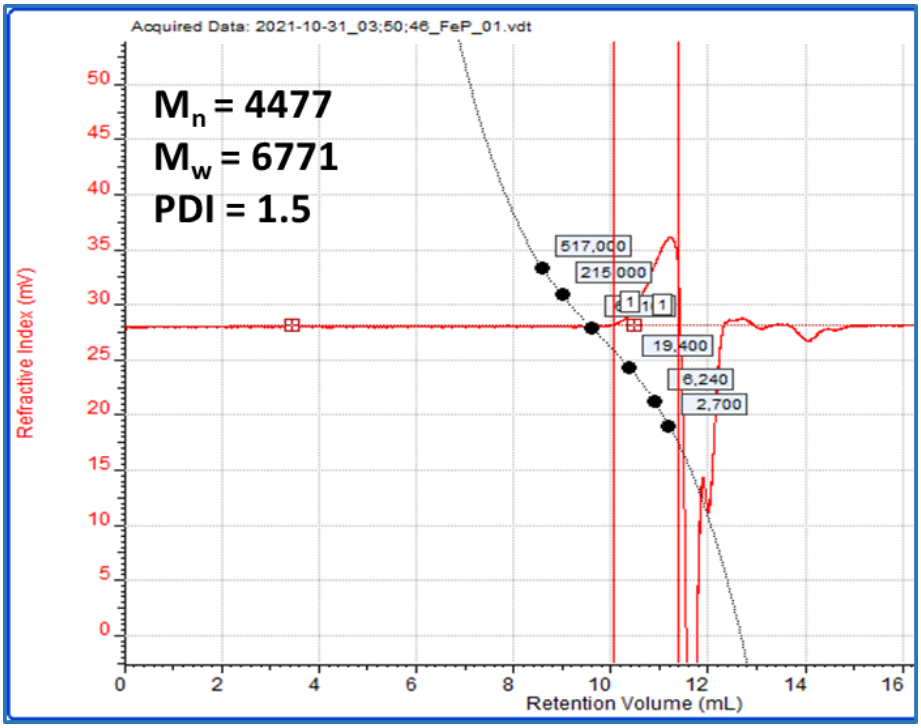

5. Self-assembly of the Block copolymers:

Preparation of vesicles: Individual stock solutions of the polymers **P-*b*-C** and **P-*b*-F** was prepared in DMF by dissolving 1.3 mg of the polymer in 125 µL of DMF. 5 µL of the aliquot from either of **P-*b*-C** or **P-*b*-F** in DMF was further diluted with deionized water to 1 mL, followed by overnight incubation with slow stirring to achieve vesicles **P-*b*-C** or **P-*b*-F** in 0.5%v/v DMF in water.

Preparation of co-assemble vesicles: Stock solutions of the polymers was prepared in DMF by mixing **P-*b*-C** (1.3 mg) and **P-*b*-F** (1.3 mg) of the polymer in 250 µL of DMF. 5 µL of the DMF aliquot was further diluted with deionized water to 1 mL, followed by overnight incubation with slow stirring to achieve co-assembled vesicles of **P-*b*-C** and **P-*b*-F** in 0.5%v/v DMF in water.

6. Polymer chain collapse by photodimerization:

(A) Monitoring photodimerization by UV spectroscopy: The polymer solution of **P-*b*-C** DMF (0.5% v/v) in water (0.01 mM) was irradiated with UV_B light (λ_{max} = 320 nm) that showed a gradual decrease in the characteristic absorption of the coumarin over 60 min. The percentage degree of photodimerization was calculated according to formula $\%PD = (A_o - A_t)/A_o * 100$ where A_t is the absorbance at time t and A_o is the initial absorbance.

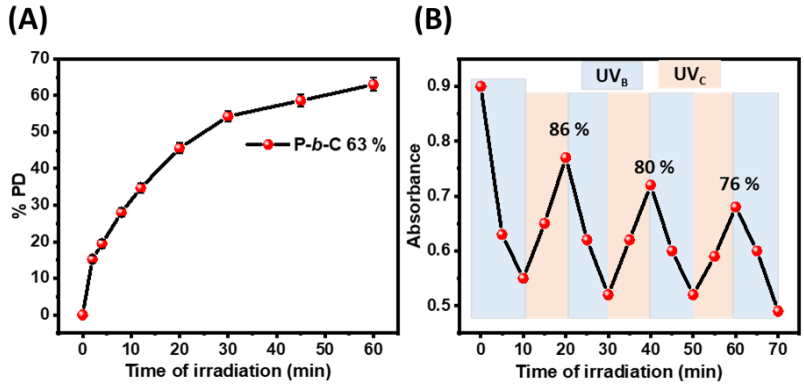

Fig. S1: (A) Photodimerization degree (PD) of **P-*b*-C** after UV_B irradiation for 60 min (UV_B lamp 1*8W). (B) Photoreversible nature of **P-*b*-C** upon consecutive irradiations with UV_B and UV_C to monitor the change in %PD values.

The kinetics of the photodimerization was monitored using %PD values in equations of First (1) and Second-order rate law (2).

$$ln(1/(1-PD) = k_1t \ldots\ldots\ldots (1)$$

$$1/(1-PD) = ck_2t+1 \ldots\ldots\ldots (2)$$

where c the initial effective concentration (0.01 mM) of the coumarin groups, k_1 and k_2 are rate constant of the first and second order kinetics of photodimerization. The polymer **P-*b*-C** exhibited higher regression coefficients for the second-order plots than those of the first-order ones confirming second order kinetics for photodimerization with a rate constant value 2.8 x 10^2 ($mM^{-1}min^{-1}$) and regression coefficients value of 0.90.

(B) Monitoring chain collapse by DLS: DLS measurements were performed on Malvern Zetasizer Nano ZS ZEN3600 equipped with a Helium-Neon laser (λ= 633 nm with backscattering angle of 173°). Aqueous solution of **P-*b*-C** with DMF (0.5% v/v) in water (0.001 mM) was filtered through 0.2 μm PTFE-filter in a glass cuvette with a path length of 1 cm. The samples were irradiated with UV_B light for 60 min and were analysed by DLS.

7. Polymer chain collapse by host-guest complexation:

(A) Monitoring host-guest complexation of by UV spectroscopy: The polymers **P-*b*-C** or **P-*b*-F** with DMF (0.5% v/v) in water (0.01 mM) and **bis-β-CD** (2 mM) were taken in HPLC water. Job's plot was constructed by varying the molar ratio of **P-*b*-C** or **P-*b*-F** to **bis-β-CD** from 0 to 1 keeping the total concentration of **P-*b*-C** or **P-*b*-F** constant at 0.01 mM. The stoichiometry of the **P-b-C⊂bis-β-CD** complex was meticulously maintained with **P-b-C** having 10 coumarin units and **bis-β-CD** comprising 2 β-CD moieties led to a 1:1 stoichiometric ratio with respect to the functional motif responsible for host-guest complexation.

Binding constant was determined monitoring the increase in absorbance at 300 to 350 nm on titration with gradual addition of 2 mM **bis-β-CD** at 2 μL per injection. The reciprocal plot of change in absorbance (ΔA) of **P-*b*-C** or **P-*b*-F** against the concentration of **bis-β-CD** was fitted using non-linear least square equation to obtain binding constant value.

$$\Delta \boldsymbol{A} = \mathbf{1/2}\ \{\boldsymbol{\varepsilon}([\boldsymbol{H}]_o + [\boldsymbol{G}]_o + \mathbf{1}/\boldsymbol{K_a}) \pm (\boldsymbol{\varepsilon}^2([\boldsymbol{H}]_o + [\boldsymbol{G}]_o + \mathbf{1}/\boldsymbol{K_a})^2 - \mathbf{4}\boldsymbol{\varepsilon}^2[\boldsymbol{H}]_o[\boldsymbol{G}]_o)^{1/2} \ldots\ldots (11)$$

Where ΔA is the chemical shifts change of **P-*b*-C** or **P-*b*-F** upon addition of **bis-β-CD** as $\Delta A = A_{(\text{with bis-β-CD})} - A_{(\text{without bis-β–CD})}$, ε is the sensitivity factor, and $[H]_o$ and $[G]_o$ are the initial concentrations of **bis-β–CD** and **P-*b*-C** or **P-*b*-F**, respectively.

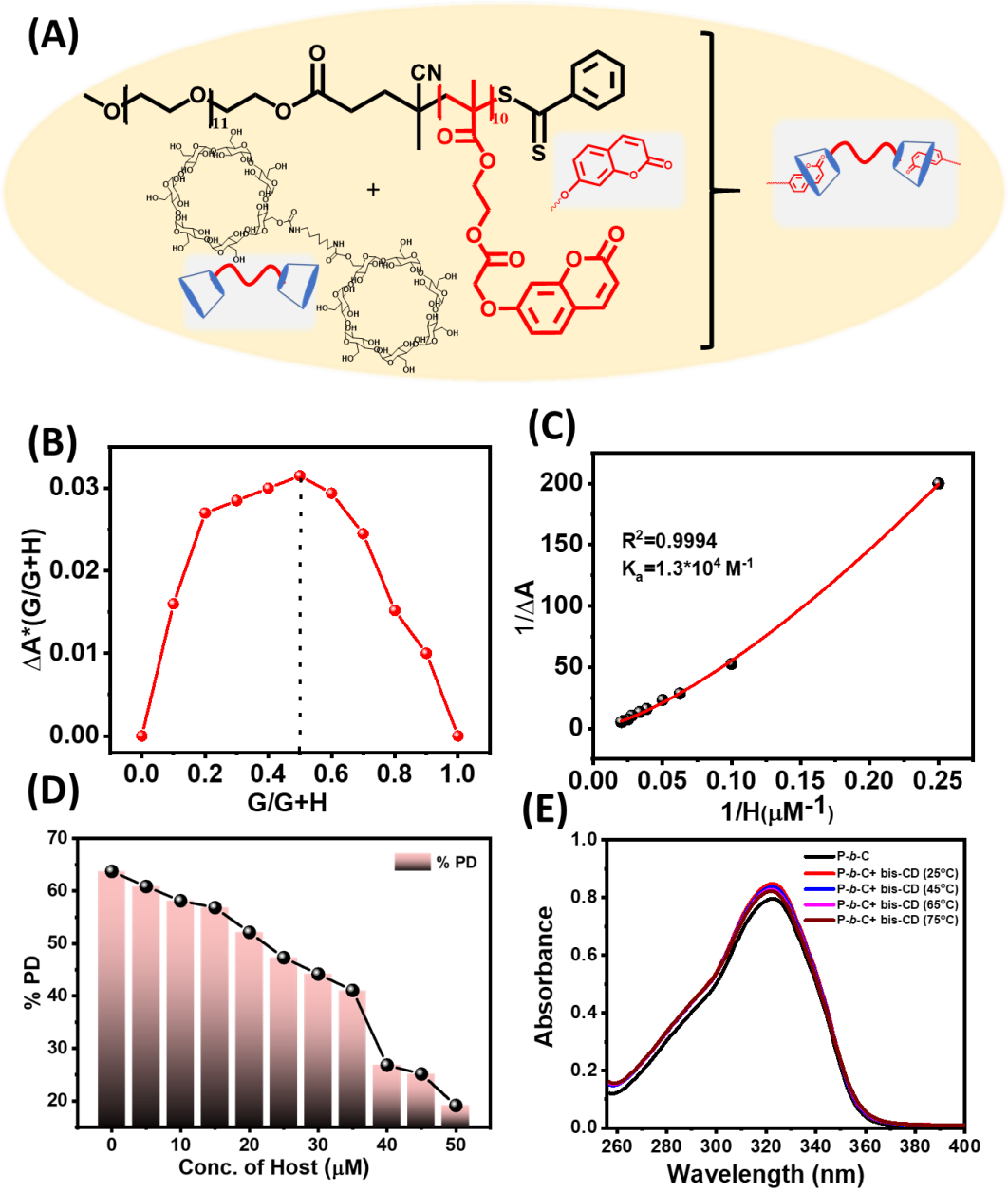

Fig. S2: (A) Structural details depicting host-guest interaction of coumarin moieties of **P-*b*-C** inside **bis-β-CD** crosslinker to form inclusion complex. (B) Job's plot of **P-*b*-C** against **bis-β-CD** showing 1: 1 complexation stoichiometry. (C) Determination of the binding constant from increase in absorbance upon titrating 0.01 mM **P-*b*-C** with **bis-β-CD**. (D) Effect of host **bis-β-CD** concentration over the photodimerization degree showing a decrease with host concentration. (E) Thermal decomplexation of the inclusion complex of **P-*b*-C** with **bis-β-CD** upon increasing temperature [**P-*b*-C**]= 0.01 mM, [**bis-β-CD**]= 0.05 mM.

Thus, Fig. S2E showed increase in absorbance in the wavelength range of 320 nm upon complexation of **bis-β-CD** with **P-*b*-C**. However, upon heating the complex up to 75 °C, we could observe some decrease in absorbance indicating partial decomplexation. However, it is noteworthy that high cooperativity of the decomplexed coumarin motifs in **P-*b*-C** polymer resulted in complexation upon cooling. Thus, such thermal decomplexation could not be probed by TEM images as it was feasible with addition of competitive guest like Ada to result chemical cue mediated decomplexation. Similarly, Fig. S3D showed increase in absorbance in the wavelength range of 450 nm upon complexation of **bis-β-CD** with **P-*b*-F**. However, upon heating the complex upto 75 °C, we could observe some decrease in absorbance indicating partial decomplexation.

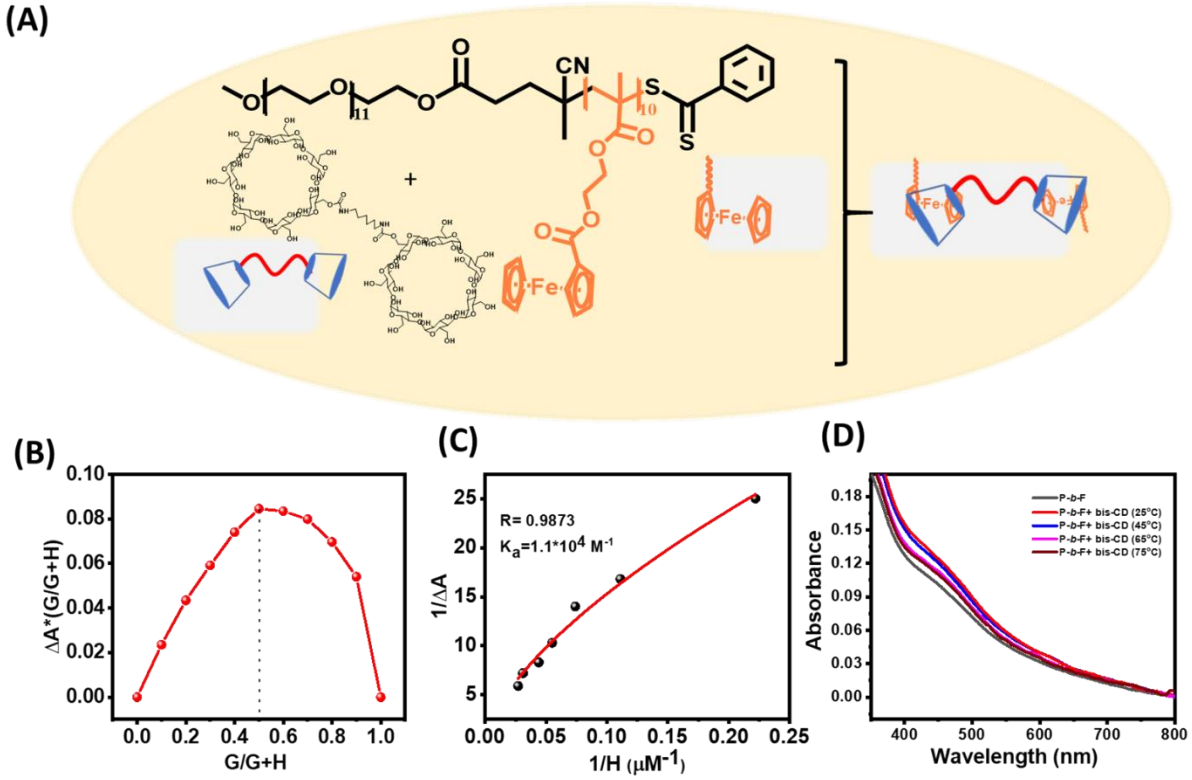

Fig. S3: (A) Structural details depicting host-guest interaction of ferrocene moieties of **P-*b*-F** inside **bis-β-CD** crosslinker to form inclusion complex. (B) Job's plot of **P-*b*-F** against **bis-β-CD** showing 1: 1 complexation stoichiometry. (C) Determination of the binding constant from increase in absorbance upon titration of **P-*b*-F** (0.01 mM) with **bis-β-CD**. (D) Thermal decomplexation of the inclusion complex of **P-*b*-F** with **bis-β-CD** upon increasing temperature. [**P-*b*-F**]= 0.01 mM, [**bis-β-CD**]= 0.05 mM.

(B) Monitoring host-guest complexation by ^{1}H-NMR: DMSO-d_6 solution of the polymers **P-*b*-C** or **P-*b*-F** (2.7 mM) was mixed with 13 mM **bis-β-CD**. It is notable that in DMSO the polymers did not self-assemble to form vesicles. We monitored the characteristic shift in proton peaks that are responsible for the host-guest complexations.

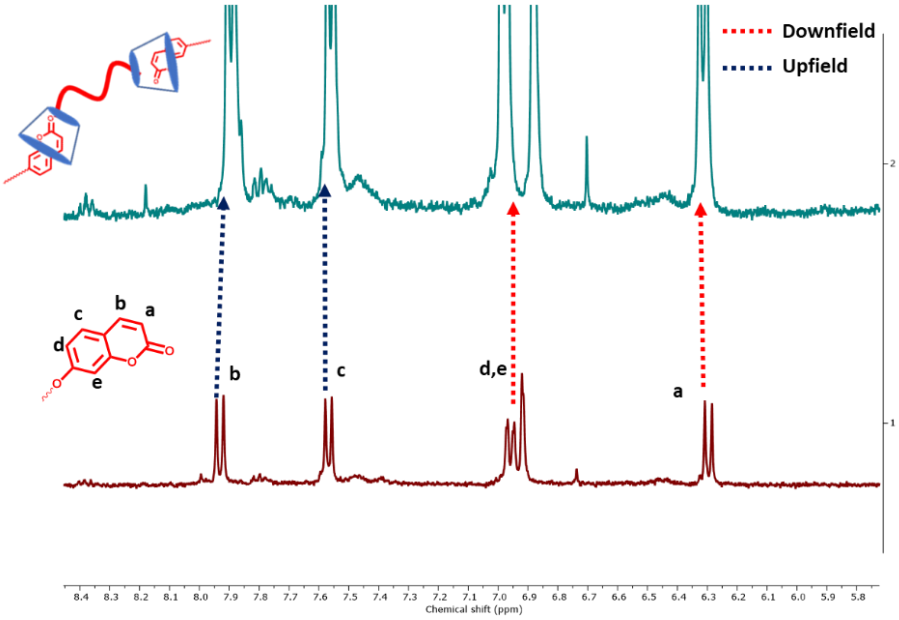

Fig. S4: ^{1}H NMR spectra showing shift of proton signals of polymer **P-*b*-C** on addition of 5 eqv. of **bis-β-CD.** *b* and *c* showed upfield shift due to the shielding effects on coumarin inside cyclodextrin cavity environment. [**P-*b*-C**] = 2.7 mM, [**bis-β-CD**] =13 mM.

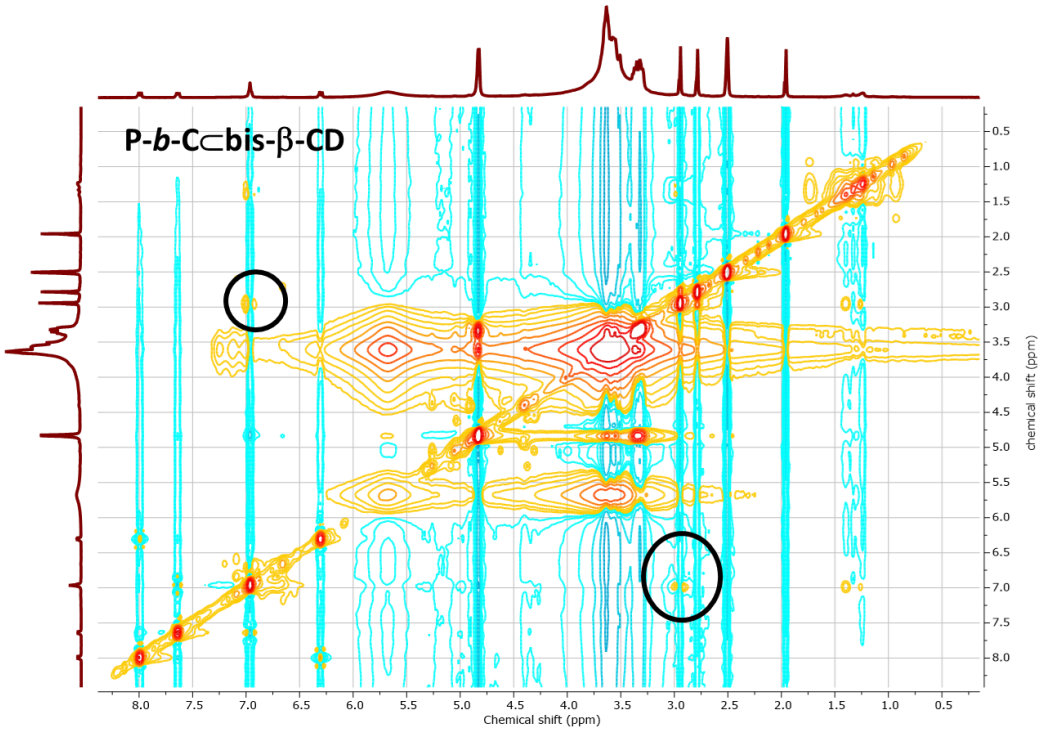

Fig. S5: 2D NMR ^{1}H–^{1}H NOESY (400 MHz) analysis of polymer **P-*b*-F** with **bis-β-CD** showing presence of cross contour peaks. [**P-*b*-C**] = 2.7 mM, [**bis-β-CD**] =13 mM.

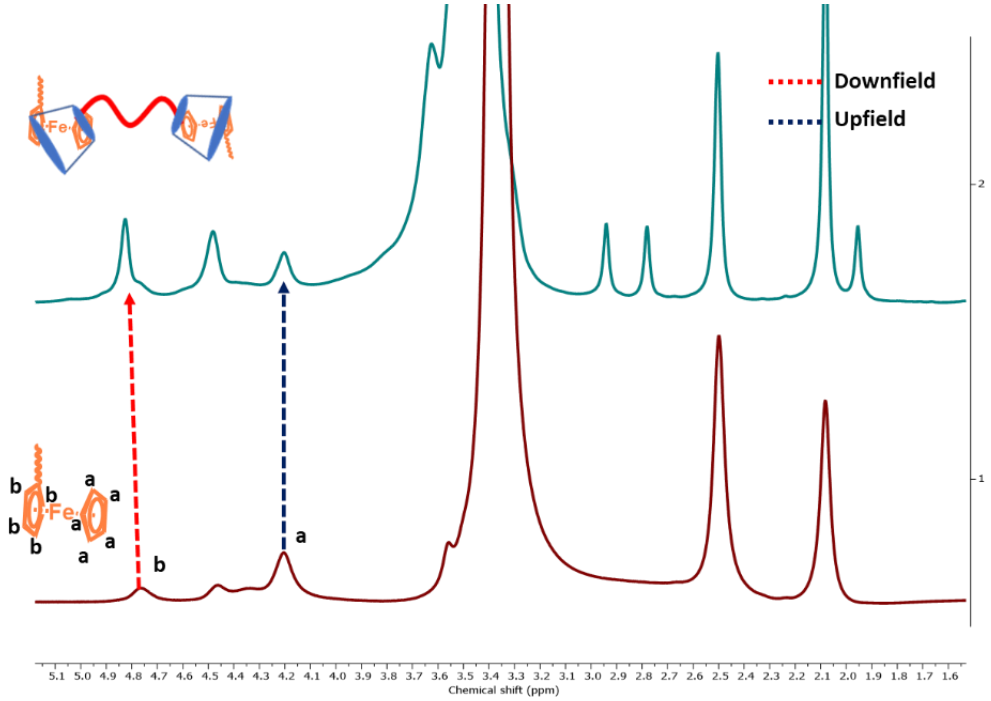

Fig. S6: ^{1}H NMR spectra showing shift of proton signals of polymer **P-*b*-F** on addition of 5 eqv. of **bis-β-CD.** *a* showed upfield shift and *b* showed downfield shift due to the shielding effects on ferrocene inside cyclodextrin cavity environment. [**P-*b*-F**] = 2.8 mM, [**bis-β-CD**] =13 mM.

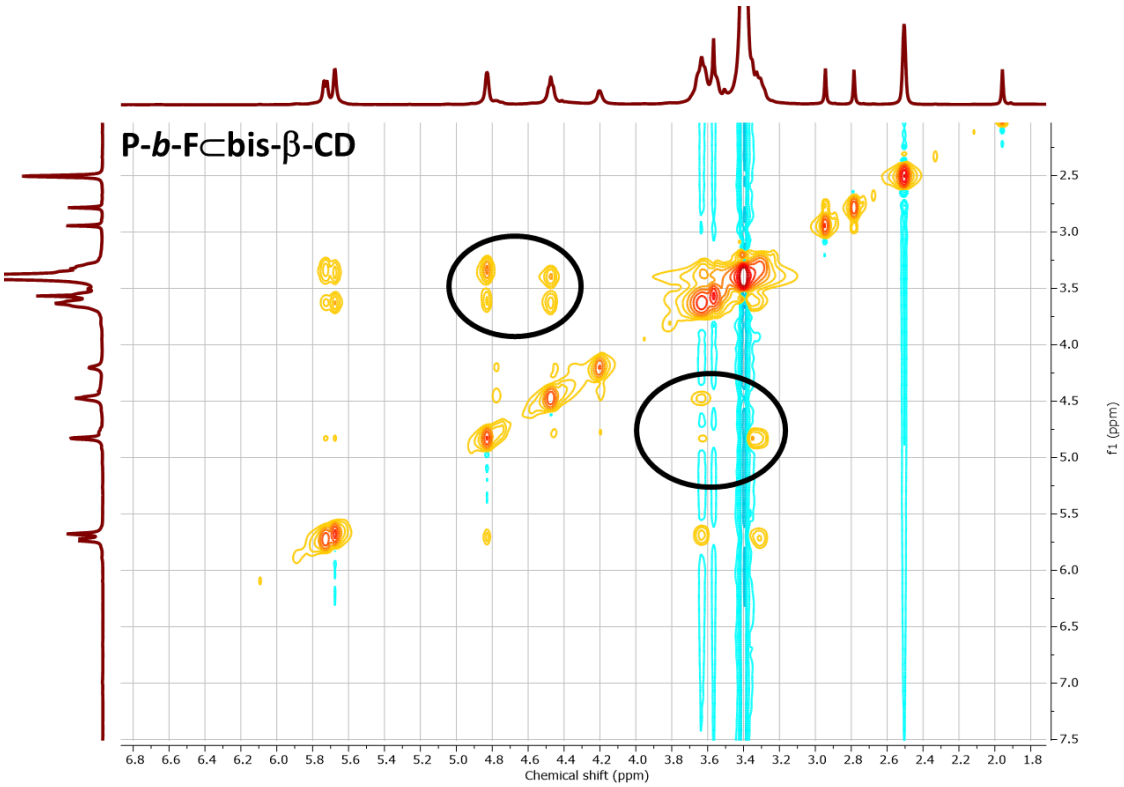

Fig. S7. 2D NMR ^{1}H–^{1}H NOESY (400 MHz) analysis of polymer **P-*b*-F** with **bis-β-CD** showing presence of cross contour peaks. [**P-*b*-F**] = 2.8 mM, [**bis-β-CD**] =13 mM.

8. Redox responsive behaviour of polymer:

Stock solutions of $Fe(ClO_4)_3$ (3 mM) and ascorbic acid (3 mM) were prepared. For oxidation, one equivalent of $Fe(ClO_4)_3$ added to polymers **P-*b*-F** with DMF (0.5% v/v) in water (0.01 mM) and analysed using UV spectroscopy. For reduction, 1 equivalent of ascorbic acid was added to the same polymer solution.

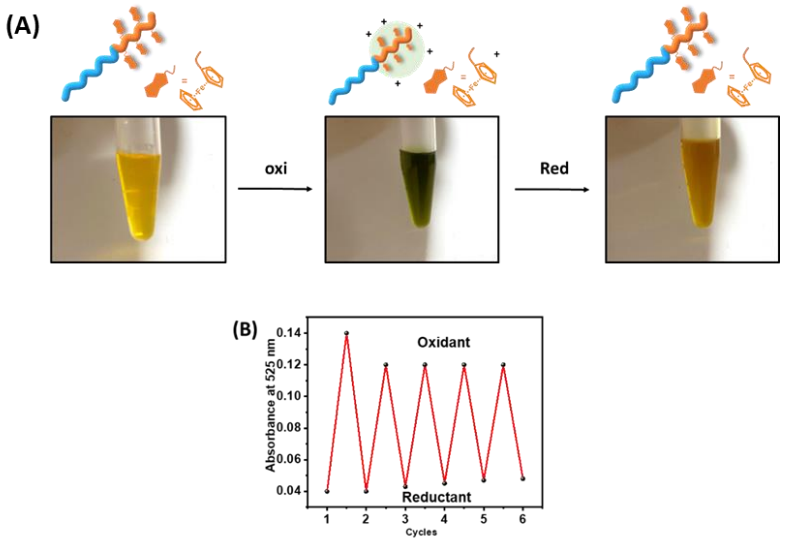

Fig. S8: Redox-responsiveness of the ferrocene grafted polymer **P-*b*-F**. (A) Colour changes to dark green after addition of the oxidising agent $Fe(ClO_4)_3$ that could be reverted back to original form upon addition of ascorbic acid. (B) Consecutive oxidation and reduction cycles for polymer **P-*b*-F**.

9. Stimuli-responsive structural transformation:

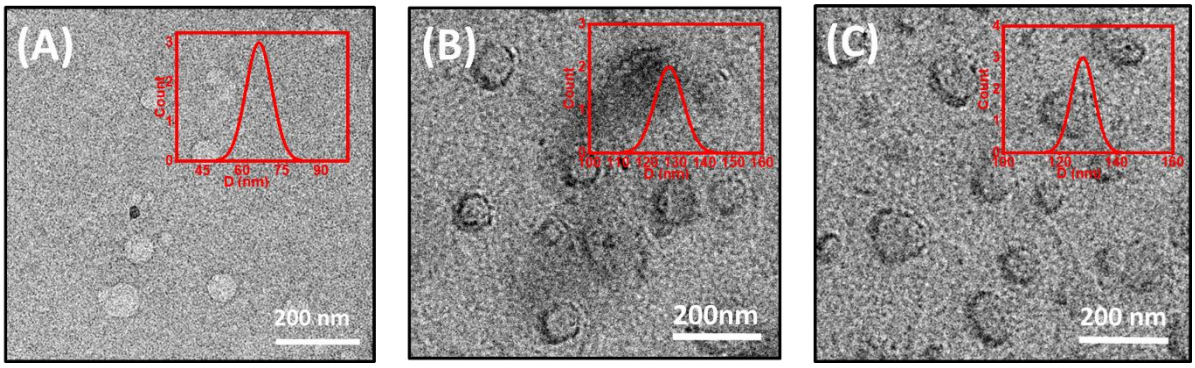

Fig. S9: (A) TEM image showing micelles for **P-*b*-F** after addition of **bis-β-CD** via host-guest interaction. Reversible nature of structural transformation to reform the vesicles upon (B) addition of reducing agent (ascorbic acid), (C) addition of competitive guest (Ada). [**P-*b*-F**] = 0.001 mM, **bis-β-CD** = 0.005 mM**,** ascorbic acid = 0.01 mM.

Our study with the **P-b-C** vesicles from the low molecular weight polymers of M_n ~4.5K at a relatively low concentration (0.001 mM), the tendency of chain collapse under the influence of photo-irradiation

and **bis-β-CD** could be attributed to the proximity of the coumarin moieties for kinetically faster intrachain collapse leading to the change in the packing parameter as observed in the experimental data. However, we argue that such kinetics of intrachain collapse might be modulated by polymer molecular weight to increase the reptation time, concentration and proximity of the functional groups. At higher concentration (0.01) the vesicles appeared in close proximity to each other (Fig. S10A-B).

TEM image recorded after the exposure of UV_B irradiation for **P-b-C** (c = 0.001) showed dissasmbly of vesicles (Fig. S10C).

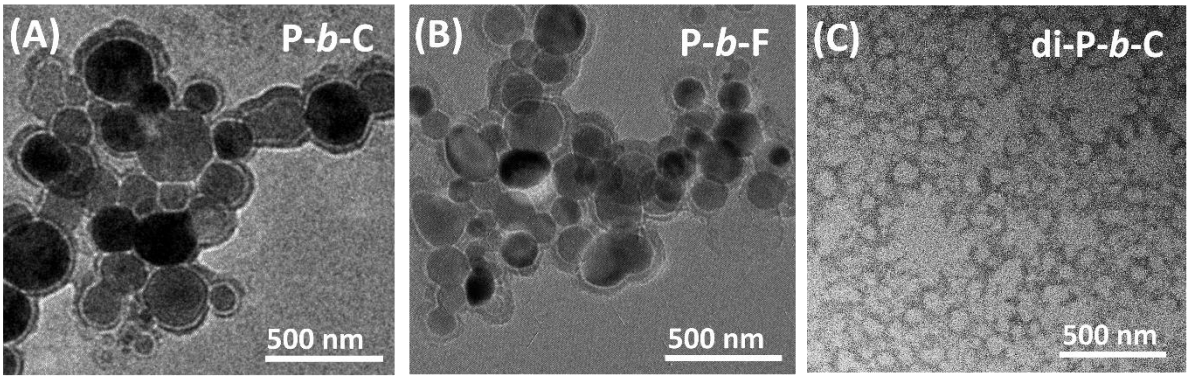

Fig. S10: TEM image showing spherical aggregation for (A) **P-*b*-C** and (B) **P-*b*-F** at higher concentration of 0.01 mM. (C) TEM images of **P-*b*-C** immediately upon exposure to UV_B irradiation showing disassembly of the vesicles (c = 0.001 mM).

10. Schemes for nanostructures formation upon polymer chain collapse:

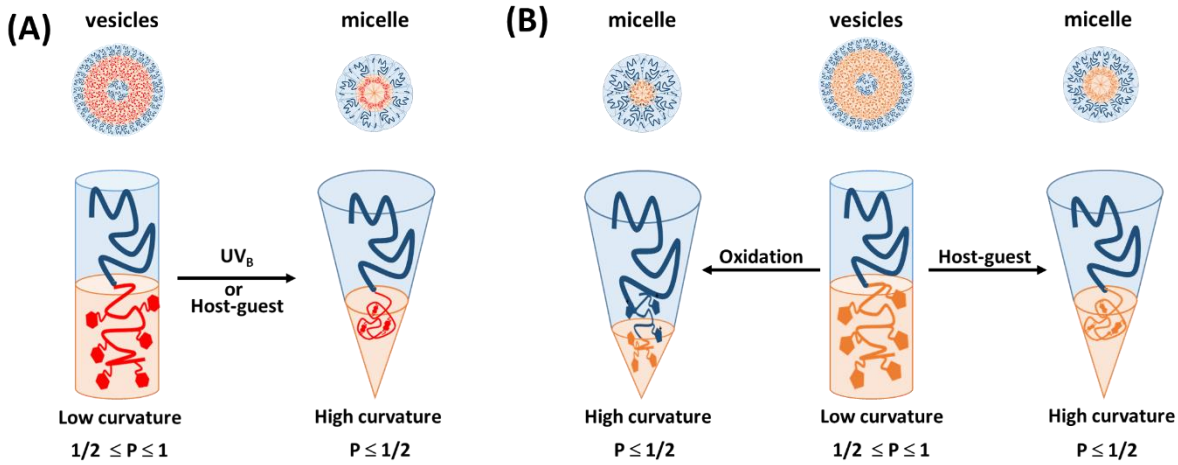

Scheme S2: Self-assembled structures formed by amphiphilic block copolymers for (A) **P-*b*-C** and (B) **P-*b*-F** with external stimuli. Inherent curvature of the block copolymer as dictated by packing parameter, *p* govern the formation of self-assembled nanostructures. Lower *p* values favour micelles and higher one is for vesicles. The chain collapse of the hydrophobic segments modulates the *p* values.

11. Monitoring orthogonal stimuli response in polymer blends:

The coassembled vesicles from the blend samples of **P-b-C** and **P-b-F** with DMF (0.5% v/v) in water (0.01 mM) exhibited characteristics UV- absorbance bands at 320 nm and 450 nm that accounted for coumarin and ferrocene motifs respectively. Upon UV_B exposure the absorbance at 320 nm drastically reduced without any visible change ~450 nm wavelength region (Fig. S11A). On the contrary, upon adding oxidant the absorbance at ~450 nm shifted towards ~650 nm that could be reverted back upon adding reducing agent, ascorbic acid (Fig. 11B). Incidentally, high absorbance of the ferrocenium ions also increase the overall absorbance in the wavelength range of ~300-400 nm where coumarin absorbs. Quite expectedly, adding chemical cue, **bis-β-CD** resulted increase in both the absorbance bands ~320 nm and 450 nm suggesting formation of the inclusion complexes (Fig. S11C).

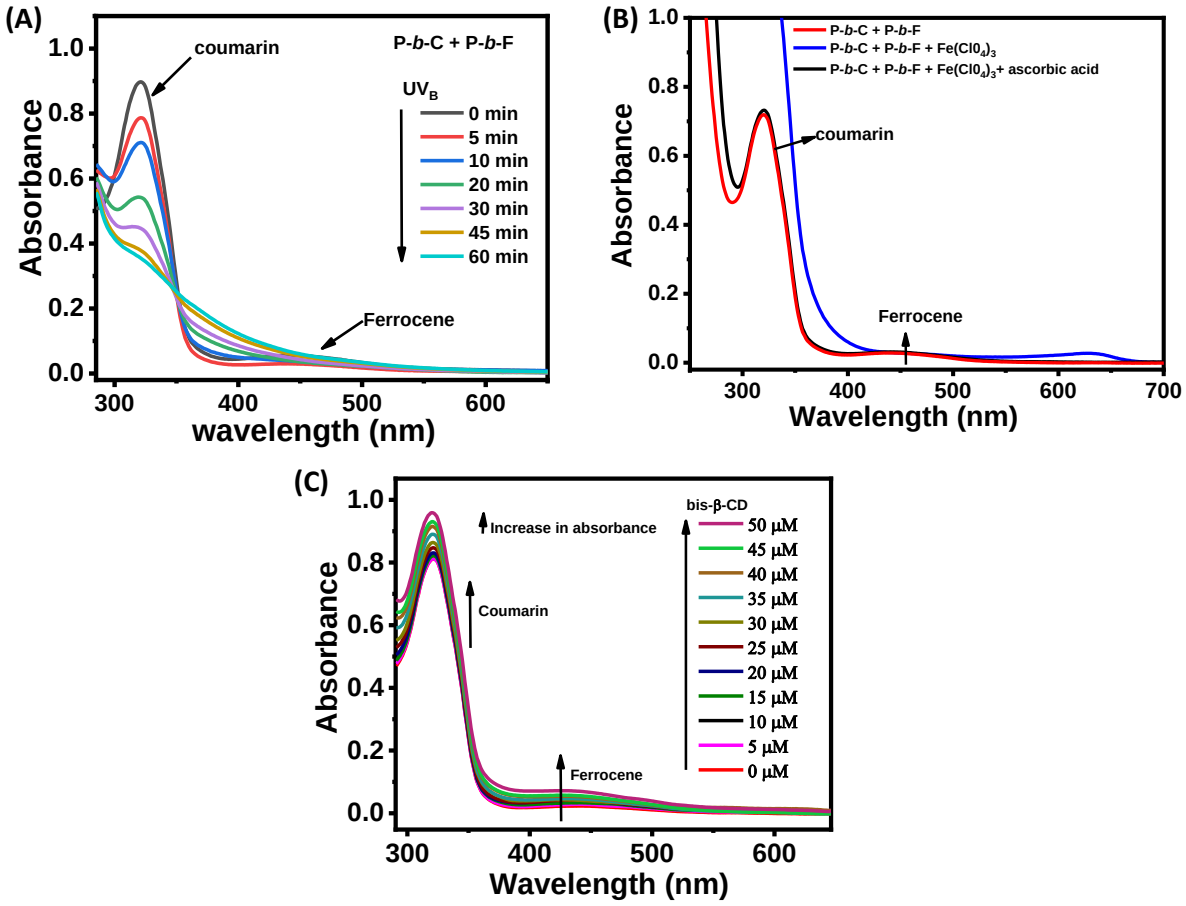

Fig. S11: UV-vis spectra for the coassembled vesicles from polymer blends of **P-*b*-C and P-*b*-F** upon exposure to (A) photo (UV_B), (B) redox ($Fe(ClO_4)_3$ and ascorbic acid) and (C) chemical (**bis-β-CD**) stimuli. [**P-*b*-F**] = 0.01 mM, [**bis-β-CD**] = 0.05 mM, [ascorbic acid] = 0.1 mM. [λ_{max} = 320 nm].

Thus, UV_B light enabled the coumarin units in **P-b-C** to undergo chain collapse of coumarin block to transform the co-assembled vesicles into micellar structures leaving **P-b-F** in its vesicles. Likewise, introduction of $Fe(ClO_4)_3$ as a redox stimulus oxidized the ferrocene in **P-b-F** to increase the

hydrophilicity of diblock polymer leading to disassembly of co-assembled vesicles. Meanwhile, **P-b-C**, being inert to this specific redox condition, maintained its vesicle morphology.

Interestingly, we found that immediately after the exposure to the stimuli, coassembled vesicles (Size ~125 nm) from the polymer blend of **P-b-C** and **P-b-F** formed mixture of transformed micelles (Sizes ranging from ~55 to 70 nm) and vesicles (Sizes from ~55 to 70 nm). However, upon keeping the sample unagitated overnight the vesicles increases in size to ~120-125 nm. This might suggest the disassembled monomer are in dynamic equilibrium with the self-assembled structures and eventually leads to optimization to the size of the self-sorted vesicles comparable to the original vesicles of **P-b-C** and **P-b-F**.

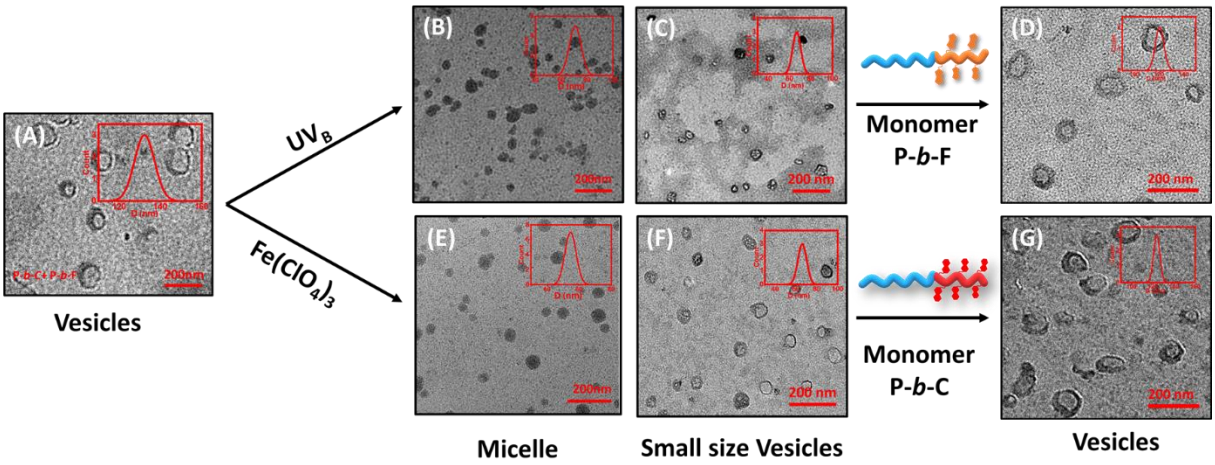

Fig. S12: (A) TEM image of the co-assembled vesicles of **P-*b*-C** and **P-*b*-F.** Transformation of the coassembled vesicles under UV_B light to (B) micelles (~55 nm), (C) small size vesicles (~60 nm) that further matures to (D) larger vesicle (~120 nm), and under redox cue, **$Fe(ClO_4)_3$** to furnish (E) micelles (~68 nm), (F) small vesicles (~60 nm) that further matures to (G) larger vesicles (~125 nm).

12. References:

[S1] W. L. F. Armarego and D. D. Perrin, Purification of laboratory chemicals (4th edition), Butterworth-Hienemann educational and professional publishing ltd, 1996, pp. 15-16.

[S2] H. Gao, Y. Tang, Z. Hu, Q. Guan, X. Shi, F. Zhu and Q. Wu, *Polym. Chem.*, 2013, **4**, 1107-1114.

[S3] D. Bogdal and M. Galica, *Pure Appl. Chem.*, 2019, **91**, 497-508.

[S4] Z. Gao, J. Zhang, K. Li, D. Lan, Z. Zhao and K. Kou, *J Mater Sci. Mater. Electron*, 2020, **31**, 10437-10445.

[S5] P. Shi, H. Zhou, C. Gao, S. Wang, P. Sun and W. Zhang, *Polym. Chem.*, 2015, **6,** 4911-4920.